



ELSEVIER

Surface Science 387 (1997) 167–182

surface science

Effect of kinks and concerted diffusion mechanisms on mass transport and growth on stepped metal surfaces

J. Merikoski^{a,b,c,*}, I. Vattulainen^{a,b}, J. Heinonen^a, T. Ala-Nissila^{a,b,d}

^a Helsinki Institute of Physics, PO Box 9 (Siltavuorenpenger 20 C), FIN-00014, University of Helsinki, Helsinki, Finland

^b Department of Physics, Box 1843, Brown University, Providence, RI 02912, USA

^c Department of Physics, University of Jyväskylä, PO Box 35, FIN-40351 Jyväskylä, Finland

^d Laboratory of Physics, Tampere University of Technology, FIN-33101 Tampere, Finland

Received 3 February 1997; accepted for publication 1 April 1997

Abstract

We study the effect of kinks and concerted atomic mechanisms on diffusion processes relevant to metal-on-metal homoepitaxy on fcc metal surfaces vicinal to the fcc (100) direction. First, we carry out extensive finite-temperature molecular dynamics simulations based on the effective medium theory to search for diffusion mechanisms that dominate the mass transport perpendicular and parallel to step edges. Then, the energetics of these processes are studied by ground state calculations. Our results show that kinks play an important role for diffusion both across and along step edges. In particular, the combined effect of kinks and concerted exchange is found to be able to remove locally the step edge barrier for mass transport across the step. The relative importance of some of the processes depends on the local tilt of the interface. We report results for copper, silver, and nickel, and discuss the generic features of energetics of diffusion processes in effective medium theory and other semi-empirical many-atom models. We also consider the implications of our results on surface growth and for models of surface growth under molecular beam epitaxy conditions. © 1997 Elsevier Science B.V.

Keywords: Computer simulations; Growth; Stepped metal surfaces; Surface diffusion

1. Introduction

Migration of adatoms and molecules is one of the most fundamental microscopic processes taking place on solid surfaces. It plays a key role in many phenomena, such as catalysis, ordering and crystal growth, that are important for practical applications [1,2]. In many cases the resulting macroscopic properties often depend on the atomistic details of diffusion processes [2]. Thanks to modern experimental tools, such as the field ion

microscope [3] and the scanning tunnelling microscope [4], as well as progress on the theoretical side [5], true microscopic information about adatom dynamics has become available. Despite this, there are many cases where the microscopic nature of the diffusion processes is still under intense study. One such case of particular interest is the so-called exchange mechanism, which is now known to be an important, and in some cases the dominant, factor in mass transfer on smooth metal surfaces [6–8].

In practice, however, metallic surfaces are seldom smooth but may contain a high density of atomic steps. Steps are also naturally created

* Corresponding author. E-mail: merikosk@csc.fi

during growth on low index surfaces. Recently, diffusion on stepped surfaces has been studied both experimentally [9] and theoretically [10,11]. These studies reveal that steps can, in some cases, cause significant changes in the values of the diffusion coefficients of adatoms compared with smooth surfaces. From a microscopic point of view, one of the central issues is the possible existence of an effective Schwoebel or step edge barrier [12]. The role of this barrier is to prevent or slow down migration of adatoms across step edges. It is easy to understand qualitatively, and can be shown by a theoretical analysis [13,14] that, under typical molecular beam epitaxy (MBE) conditions, the step edge barrier can lead to a growth instability. This is expected to be the case at temperatures much lower than the step edge barrier, where simple hopping mechanisms are inefficient for mass transport across steps. In this case, the importance of mechanisms other than the simple hopping lies in the possible reduction of the step edge barrier. Exchange or many-particle concerted processes at step edges may thus not only enhance diffusion rate on the surface, but also change the whole morphology of a growing surface.

Apart from steps, another feature characteristic of growing surfaces is the high density of kinks at step edges. While the step edge barrier and its implications on growth have been studied in various systems with straight step edges [15,16], the effect of kinks has received considerably less attention. The aim of the present work is to consider microscopic details of diffusion in the vicinity of steps and kinks, the main emphasis being in the combined effect of kinks and exchange-type mechanisms on diffusion at step edges. To find the dominant diffusion mechanisms at step edges we have carried out extensive finite-temperature molecular dynamics (MD) simulations for a model of vicinal fcc (11 \bar{m}) surfaces, where the metallic interactions between atoms have been derived from the effective medium theory (EMT) [17]. In the present work we concentrate on copper, silver and nickel as representative examples of fcc metals. The activation barriers of the relevant processes are then obtained from ground-state calculations. For flat surfaces and straight step edges, our results

are compatible with data from phenomenological methods [18–30]. Our results show that exchange processes and concerted mechanisms at kink sites play a crucial role in reducing the existing step edge barrier. Also, kinks are important for mass transport along the step edges. We discuss the implications of these results for surface growth, and their reliability in light of recent first-principles calculations [31–34] and experimental work [35–49].

2. Model and methods

The calculation of activation barriers of diffusion processes requires the evaluation of the total energy, which in turn requires a description of interparticle interactions. To this end, the most concise approach at present is the density-functional theory (DFT) [50]. However, the full DFT, as well as its approximations such as the local density approximation (LDA) and generalized gradient approximations (GGA) [51], are not yet feasible for studies of systems with very large unit cells and phenomena with long characteristic time scales. While some studies of diffusion processes using these sophisticated methods have recently been carried out [33], many of the problems considered in the present work are still beyond reach with them. The most commonly used phenomenological approximations are the embedded atom method (EAM) [52], tight binding (TB) [53] and Finnis–Sinclair (FS) [54] methods, the glue model [55], and the EMT [17]. In these various phenomenological methods, some many-atom effects are included using parameterized functional forms for the dependence of the energy of an atom on the distance from the neighbouring atoms, with a resulting expression for the total energy of a metallic system of the generic form

$$E_{\text{tot}} = \sum_i F(\rho_i) + \sum_{j \neq i} V(|r_i - r_j|) \quad (1)$$

where r_i is the position of the atom i , F is some non-linear function of a local quantity ρ_i characterizing the environment of that atom, and V is a pair potential. In the present work we have chosen to use the EMT method, which in the form used

here is the one least based on experimental data. Within EMT, ρ_i has an interpretation as a superposition of atomic electron densities ρ due to neighbouring atoms, $\rho_i = \sum_{j \neq i} \rho(|r_i - r_j|)$. Although the EMT is not comparable to first-principles methods with regard to quantitative accuracy, it has still been applied successfully to many surface problems, such as surface relaxation [17], surface melting and roughening [56–59], reconstruction [60,61], diffusion [22,62–64], and deposition of atoms on islands [62]. Thus, we feel that its use in the present context is justified.

The parameterization of the EMT as used here is based on LDA studies by Puska [65], unless otherwise stated. We use the “basic” EMT without the so-called one-electron correction [17]. Here we shall not describe the EMT formalism or the underlying physics in detail; a recent summary can be found in Ref. [66]. The numerical implementation of EMT as used in our studies is described by Häkkinen and Manninen in Ref. [57]. For each metal studied, we first determined the thermal expansion curves needed in our NVT simulations by using the methods described, for example, in Ref. [67]. In the NVT simulations with the Nosé–Hoover thermostat [68,69], a typical system size was 2800 atoms with ten dynamic layers on top of four static layers. The length of the time step was chosen to be well below the maximum time step that conserved the energy when the thermostat was not applied. The relaxation time parameter of the thermostat was chosen to make sure that the system remained canonical during the simulations [70]. To sample various diffusion mechanisms at step edges within the NVT ensemble, an initial configuration with a vicinal fcc (11 \bar{m}) surface was created with additional adatoms on terraces, and the system was let to evolve over time periods of the order of 10 ns, which in the case of copper corresponds to 10^6 time steps per particle.

In the present work the NVT simulations were only used to study the qualitative features¹ of mass transport at step edges, i.e. to identify the relevant

¹ For a quantitative study of the temperature dependence of the effective activation barriers and the prefactors, the microcanonical (NVE) ensemble would be a more natural choice.

processes, while all the microscopic parameters for the observed processes were determined by zero-temperature calculations. The values of the activation barriers given below thus correspond to the static adiabatic energy barrier without the coupling to the phonon bath which tends to lower the effective barrier at higher temperatures [27].² For each diffusion process, the energy at the initial state $E^{(i)}$ (and that of the final state $E^{(f)}$) was determined by quenching from the configuration based on bulk-terminated atom positions into the relaxed zero-temperature configuration by using the velocity-quenching procedure described in Ref. [57]. To determine the energy of the lowest saddle point $E^{(s)}$, the system was taken over it by advancing one coordinate of one atom in small steps (typically $\frac{1}{50}$ of the nearest-neighbour distance) while all the other degrees of freedom were allowed to relax fully with respect to this constraint. The activation barrier of a given mechanism M is then $E_M = E_M^{(s)} - E_M^{(i)}$, and that of the reversed process $E_M^{rev} = E_M^{(s)} - E_M^{(f)}$. For some single-particle jump mechanisms we also determined the prefactor v_M of the Arrhenius-type jump rate $\Gamma_M = v_M \exp(-E_M/kT)$ using the transition state theory (TST) [72]. Within the harmonic approximation [72], the prefactor for a process M involving a jump of a single atom can be written as $v_M = v_1^{(i)} v_2^{(i)} v_3^{(i)} / v_1^{(s)} v_2^{(s)}$, which is composed of the eigenfrequencies of that atom in the initial and the saddle-point configurations. The eigenfrequencies needed here were determined by diagonalizing the 3×3 force matrix obtained by numerical differentiation of the adiabatic potential surface experienced by the hopping atom at zero temperature (see Ref. [73] for more details and an application to surface diffusion).

3. Results

We shall divide the discussion of the microscopic diffusion mechanisms into three parts: processes

² We should also note that in the low friction limit of the diffusing adatom the effective barrier is not simply determined by the adiabatic potential; for a detailed discussion and analysis see Ref. [71].

taking place on terraces (denoted by T), at straight steps (S), and involving kinks (K). Processes within these categories are then further classified on the basis of the nature of diffusion mechanism: conventional hopping events (H), simple exchanges (X), and diffusion through the motion of vacancies (V). The only exceptions to this rule are the diffusion processes that involve more than two atoms. Such “exotic” mechanisms are considered separately in Section 3.4 and denoted simply by E.

To understand the energetics of diffusion processes on surfaces vicinal to the fcc (100) direction, it is useful to consider the geometry at the atomic level of the fcc (119) surface as shown in Fig. 1. An ideal fcc (11 m) facet consists of (100) terraces of width $(m-1)r_{nn}/2$ separated by (111) steps of height $r_{nn}/\sqrt{2}$, where $m \geq 3$ is an odd integer and r_{nn} is the nearest-neighbour distance. The characteristics of diffusion mechanisms on these surfaces differ essentially from those available on surfaces vicinal to the fcc (111) direction (see e.g. Refs. [62, 74]). First, adatoms on the (100) terraces have

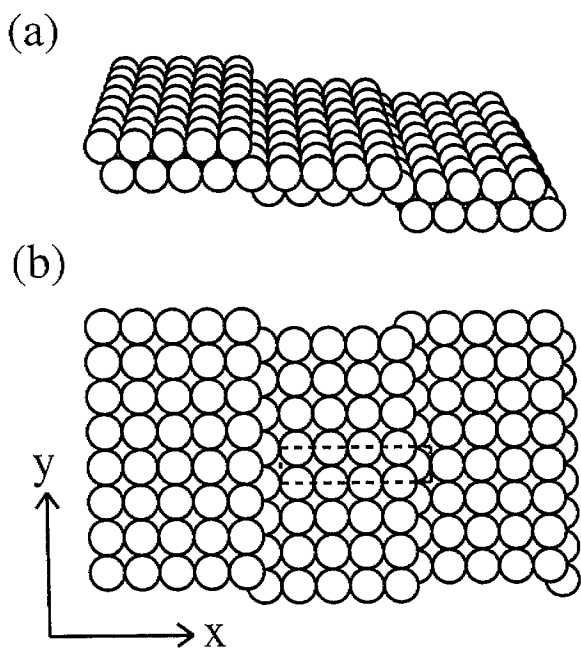


Fig. 1. The geometric structure of an ideal fcc (119) surface: (a) perspective view, and (b) top view. The size of the unit cell is shown by a dashed line.

four nearest neighbours and relax deep in the hollow site, almost inside the surface, which leads to relatively large activation energies for jump mechanisms. Second, the terraces themselves are rather loosely packed so that surface atoms within the first layer have more room to slide with respect to each other than on close-packed surfaces. Therefore, exchange mechanisms can be expected to play an important role in mass transport. The third feature is that all steps of monolayer height with close-packed $\langle 110 \rangle$ edges are of the same type on these surfaces. In Fig. 2 we show a schematic illustration of the various diffusion processes considered in this work as well as the notation. Note from Fig. 1 that simple hops across the step

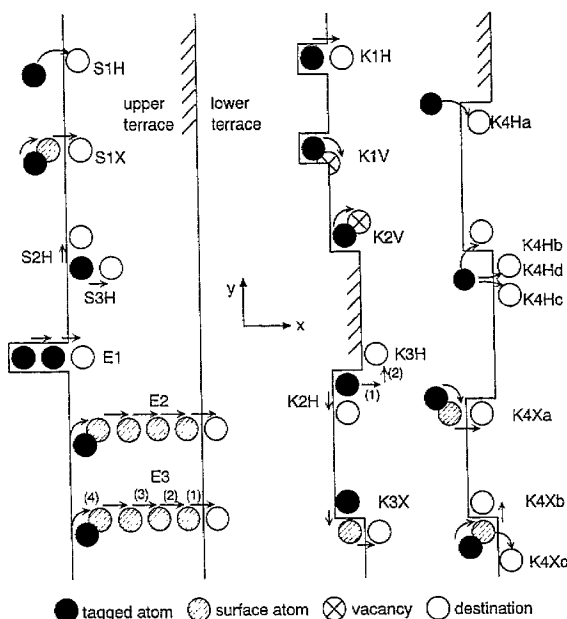


Fig. 2. Illustrative representations of the diffusion mechanisms on the fcc (119) surface studied in the present work. The classification is based on two criteria: the surface region where diffusion takes place and the diffusion mechanism responsible for mass transport in a given process. Thus, terraces are denoted by T, straight steps by S, and kinks by K. Further, the diffusion mechanisms include standard hopping events (H), exchanges (X), and diffusion through the motion of vacancies (V). Exotic diffusion events involving more than two atoms are denoted separately by E. In mechanisms denoted by X, and also in the mechanism E2, all the active atoms move concertedly at the same time. The consecutive stages of processes K3H and E3 are indicated by the numbers in parentheses (see text).

edge consists of a jump of $3r_{\text{nn}}/2$ in the x direction and a shift of $r_{\text{nn}}/2$ in the y direction.

3.1. Self-diffusion on flat (100) terraces

To compare with other results in the literature, we first consider self-diffusion on a flat (100) surface of copper, silver, and nickel. For these metals, the equilibrium adsorption site of an adatom is the four-fold hollow site. The three jump mechanisms considered here comprise a simple hopping over a two-fold bridge site (mechanism TH),³ vacancy diffusion in the first layer of the surface (TV), and the simple exchange process (TX). In the latter, diffusion occurs via an exchange of the adatom with a nearest-neighbour surface atom [6].

The results are summarized in the first part of Table 1. In the case of copper, we find an activation barrier of $E_{\text{TH}}=0.40$ eV [63] for bridge hopping. This result is in excellent agreement with other EMT [22] studies and a recent TB calculation [29], and is consistent with various EAM results, which range from 0.38 to 0.53 eV [18,20,23,25,27,28] depending on the choice of the EAM scheme. The only clear exception is the

Table 1
Activation barriers (eV) for some processes occurring on flat fcc (100) and on stepped fcc (119) surfaces with straight step edges. The barriers were evaluated from the adiabatic energy surface for each mechanism at zero temperature. Bridge hopping, exchange, and vacancy diffusion flat terraces are denoted by TH, TX, and TV respectively. For the processes at straight step edges denoted by S, see Fig. 2

M	Cu		Ag		Ni	
	E_{M}	E_{M}^{CV}	E_{M}	E_{M}^{CV}	E_{M}	E_{M}^{CV}
TH	0.399	0.399	0.367	0.367	0.631	0.631
TX	0.996	0.996	0.614	0.614	0.844	0.844
TV	0.482	0.482	0.412	0.412	0.655	0.655
S1H	0.578	0.867	0.481	0.691	0.920	1.335
S1X	0.631	0.909	0.516	0.726	0.744	1.156
S2H	0.258	0.258	0.224	0.224	0.357	0.357
S3H	0.684	0.388	0.570	0.351	1.014	0.590

³ Jumps over the four-fold atop site were found energetically very unfavorable, as expected.

value of 0.69 eV from the Car–Parrinello (CP) calculations of Ref. [31]. The basic EMT favours hopping over exchange [75], which is also the behaviour predicted by the EAM [18,20], TB [29], and CP [31] studies. However, EMT work including an additional one-electron correction [75,76] and corrected effective medium (CEM) calculations [77] predict the opposite, yielding very low values for E_{TX} . For diffusion of a single vacancy on an otherwise ideal (100) surface EMT gives $E_{\text{TV}}=0.48$ eV, which, in disagreement with EAM [25], is slightly higher than E_{TH} . On the experimental side, excluding the result of 0.28 eV by Ernst et al. [40], the data support a barrier of about 0.4 eV [37,41,42,47]. While this value seems to agree very well with E_{TH} given by basic EMT and EAM models, one must bear in mind that the actual mechanism responsible for the measured barrier has not been confirmed experimentally.

On the Ag(100) surface, we find $E_{\text{TH}}=0.37$ eV for bridge hopping. Although it agrees with other EMT studies [22], it seems to be somewhat smaller than results based on other methods. The EAM calculations give 0.48 eV [18,21,27,28,30], the results of CEM range from 0.40 to 0.46 eV [77,78], and first principles calculations give 0.50 eV [32], 0.52 (LDA), and 0.45 eV (GGA) [33]. Our result for exchange, $E_{\text{TX}}=0.61$ eV, is in reasonable agreement with previous results by EAM and CEM, which tend to values of about 0.75 eV [18,30] and 0.5 eV [77,78] respectively. The values of 0.93 eV (LDA) and 0.73 eV (GGA) based on the DFT calculations [33], on the other hand, are again higher than our corresponding result. For vacancy diffusion, we obtained the value $E_{\text{TV}}=0.41$ eV, which is in agreement with other studies [21,22]. Low-energy ion scattering measurements by Langelaar et al. [48] yielded a barrier of 0.40 eV, which, again, is close to our EMT result for E_{TH} .

For bridge hopping on nickel, we obtain $E_{\text{TH}}=0.63$ eV. This is higher than the value of 0.56 eV reported in the EMT study of Ref. [22], probably due to a different amount of experimental input in the parameterization. The CEM method predicts a barrier between 0.61 and 0.68 eV [77,78], and the EAM studies yield values ranging from 0.63 eV to 0.68 eV [18,19,26–28]. Thus our result is in reasonable agreement with previous

simulation studies. For exchange, we obtain a value of $E_{\text{TX}}=0.84$ eV. Corresponding EAM studies predict values of 0.93 eV [18,26] and 1.15 eV [18,19], while the CEM method yields 0.65 eV [78], and its modified version 1.40 eV [78] and 1.00 eV [77]. For vacancy hopping, our result $E_{\text{TV}}=0.66$ eV is close to the EAM prediction of 0.69 eV [19] and the EMT result 0.56 eV of Ref. [22]. Finally, from FIM experiments [36] and work function studies [35] the activation barrier for diffusion on Ni(100) has been estimated to be 0.63 eV and 0.60 eV respectively.

To summarize, our EMT results agree reasonably well with those given by other theoretical methods of a comparable level of sophistication. The qualitative behaviour for all the three metals is consistent with the trend $E_{\text{TH}} < E_{\text{TV}} < E_{\text{TX}}$, i.e. bridge hopping is favourable over the other available mechanisms, with the actual value of E_{TH} being close to the available experimental data for the (100) surfaces.

3.2. Self-diffusion near straight step edges

To assess the role of kinks in mass transport at step edges, we first need to consider diffusion at straight step edges. Unless stated otherwise, the results given in this and the following sections were obtained for the (11 m) surfaces with $m=9$. We have also performed calculations with $m=3$, 5, and 15. Results for the case $m=3$ will be given separately in Section 3.5.

The barriers for diffusion of a single adatom on an ideal fcc (119) surface are summarized in the second part of Table 1. The corresponding adiabatic potential energy surface in the case of Ag is shown as a contour plot in Fig. 3(a); a similar plot for copper can be found in Ref. [63]. In Fig. 3(b), in turn, we give the potential of an adatom along the optimal path across the step. A clear barrier is seen across the step edge. The edge is a strong sink, while the other barriers on the terrace are equal to E_{TH} within less than 5%. We have also verified this for Cu in the cases $m=9$ and $m=15$ [63]. At low temperatures, the slight short-range attraction of the adatom towards the ascending step edge could lead to an empty zone in front of the step,⁴ a

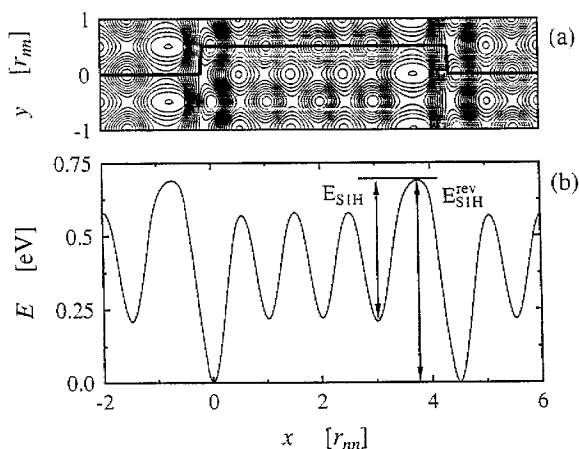


Fig. 3. (a) A contour plot of the adiabatic potential experienced by a silver adatom on an ideal Ag(119) surface as given by the EMT at zero temperature is presented. The energy difference between the adjacent contours is 0.05 eV, and the global minimum is at $(0, r_{\text{nm}}/2)$. (b) The optimal adiabatic potential for diffusion perpendicular to the straight step edge for Ag/Ag(119). The corresponding optimum route is shown by a thick line in (a).

phenomenon observed experimentally for Ni(100) [43], as well as in various other systems [80] and in a simulation study [64]. A similar weak attraction was found in the DFT calculations of Al(111) due to electronic effects [81].

An interesting question concerns the possible role of exchange in changing the value of the step edge barrier ΔE_s . In our case, we have used the definition $\Delta E_s = \min(E_{\text{S1H}}, E_{\text{S1X}}) - \min(E_{\text{TH}}, E_{\text{TX}})$. For copper and silver we obtain $E_{\text{S1H}} < E_{\text{S1X}}$, and thus the exchange plays no role at low temperatures, while for nickel the situation is opposite with $E_{\text{S1H}} > E_{\text{S1X}}$. Despite this, for all the three metals we find a non-negligible barrier with values of $\Delta E_s = 0.179$ eV (Cu), 0.114 eV (Ag), and 0.113 eV (Ni).

In the case of Cu, our result $\Delta E_s > 0$ is consistent with helium atom beam scattering experiments by Ernst et al., where a growth instability leading to a three-dimensional terrain with mounds between pyramid-like islands was observed [44,45], and X-ray diffraction studies by van der Vegt et al. [46]. It also agrees with EAM [20,25] and FS [24] calculations. For Ag, on the other hand, the intensity oscillations in reflection high-energy electron

⁴ The "empty zone" in front of an ascending step may also contribute to the growth instability, see Ref. [79].

diffraction (RHEED) during growth [39] and X-ray scattering measurements [49] indicate that growth proceeds via a two-dimensional layer-by-layer mode. Also, in recent DFT calculations by Yu and Scheffler [33,34], step-crossing at straight steps was found to occur preferentially by the exchange mechanism, with an activation barrier approximately equal to that for bridge hopping on a flat Ag(100) surface. These observations are in disagreement with our results for Ag. This supports the notion [22,25,75] that the basic EMT and other phenomenological models are not fully capable of describing the energetics of exchange mechanisms. In the case of Ni, RHEED measurements by Purcell et al. [38] and STM measurements by Kopatzki et al. [43] indicate that the growth of Ni(100) also proceeds by an almost ideal layer-by-layer mode around 300 K. This could also mean a negligible step edge barrier in contrast to our results and other EMT [22] and EAM calculations [19,26].

The process S2H, hopping along a straight step edge, is important for the morphology of growing two-dimensional islands. If the corresponding jump rate Γ_{S2H} is small in comparison with the transition rates characterizing mass transport in a direction perpendicular to the step edges, islands are expected to grow in a fractal-like manner. This is a situation typical on fcc (111) metal surfaces [81–85]. In the opposite case, islands with relatively straight steps are formed if a ledge atom can diffuse rapidly to a kink site nearby, which appears to be the behaviour on most fcc (100) surfaces [82,83,86]. Our results agree with this observed trend since, based on the activation barriers, the jump rate of adatoms along a straight step edge (SH2) is one of the fastest diffusion mechanisms considered in this work. This is in accordance with most of the previous theoretical studies for the same systems [20–23,25,26,33,35,86], and also with similar observations for other materials such as Ir(100) [87] and Rh(100) [83].

3.3. Self-diffusion near kinks on fcc (11m) surfaces

Activation barriers for diffusion mechanisms in the vicinity of kinks at step edges (denoted by K in Fig. 2) in the case of the (119) surface are given

in Table 2. We note that for an ideal, straight step, thermal kink formation is very improbable, since creating a hole via the process K1H requires crossing a high activation barrier. However, in the presence of vacancies right below the step edge, the mechanism K1V creates a hole with a very small energy cost. Thus, vacancies in the vicinity of step edges are quickly absorbed by steps.⁵

Let us now consider the effect of kinks on downwards step-crossing. For an adatom on the upper terrace in the immediate vicinity of a kink, there are seven possible ways to descend the step edge. We shall compare the energy barriers of these processes with that of the most favourable descent at a straight step edge, $E_{S1}^{\min} = \min(E_{S1H}, E_{S1X})$ and the lowest terrace barrier E_{TH} . Of the hopping processes K4Ha, K4Hb, K4Hc, and K4Hd, the most favourable one is K4Ha, with $E_{TH} < E_{K4Ha} < E_{S1}^{\min}$. Therefore, considering hopping only, kinks promote step crossing, but a clear step edge barrier persists. In the case of exchange processes K4Xa, K4Xb, and K4Xc at kink sites, the situation changes. Namely, for all the three metals, the process K4Xb has an activation barrier below the terrace barrier, i.e. $E_{K4Xb} < E_{TH}$. The reason for K4Xb to be clearly the favourable mechanism can be easily understood by simple bond counting arguments. We can conclude that, within the EMT, the step edge barrier disappears at the kink site. However, for diffusion across the step upwards via the reversed processes, the activation barrier is reduced by the kinks either not at all or only by a very small amount.

In the most favourable process K4Xb, the adatom originally on the upper terrace is absorbed by the kink, the position of which proceeds one

⁵ It is worth pointing out that for vacancies on terraces, the rate-limiting barrier to migrate onto the ascending step edge (which is the position of the vacancy in the mechanism K1V in Fig. 2) is larger than E_{TV} : in the case of Ag(119), for example, this barrier is 0.659 eV. Thus our results for K1V and K2V do not imply that vacancies on terraces are absorbed quickly by ascending step edges and kinks. Instead, it seems that vacancies on terraces tend to migrate towards the descending step edge, since the rate-limiting barrier in this direction is approximately E_{TV} . Further, bearing in mind that the barrier E_{K1V}^{rev} is small, this chain of events leads to mass transport going upwards.

Table 2

Activation barriers (eV) for some mechanisms occurring near kinks on fcc (119) surfaces and for some exotic diffusion processes (see Fig. 2). All the barriers were evaluated at zero temperature. The notion of NA corresponds to "not available" (see text footnote 6). For processes consisting of several stages the highest barrier, i.e. that of the rate-limiting step, is given

M	Cu		Ag		Ni	
	E_M	E_M^{rev}	E_M	E_M^{rev}	E_M	E_M^{rev}
K1H	0.870	0.110	0.760	0.176	1.332	0.231
K1V	0.166	0.899	0.170	0.720	0.178	1.192
K2H	0.518	0.239	0.412	0.209	0.701	0.322
K2V	0.143	0.879	0.198	0.764	0.230	1.269
K3H	0.782	0.492	0.633	0.429	1.111	0.723
K3X	NA	NA	NA	NA	NA	NA
K4Ha	0.442	1.011	0.401	0.818	0.695	1.520
K4Hb	0.451	1.011	0.409	0.816	0.751	1.518
K4Hc	0.584	0.890	0.478	0.685	0.933	1.326
K4Hd	0.584	0.860	0.478	0.672	0.933	1.326
K4Xa	0.422	1.009	0.404	0.821	0.522	1.347
K4Xb	0.378	0.938	0.323	0.731	0.471	1.240
K4Xc	0.584	0.889	0.482	0.689	0.740	1.141
E1	1.019	0.222	0.886	0.288	1.496	0.367
E2	0.870	1.074	0.760	1.032	1.332	1.731
E3	1.310	1.310	1.102	1.102	1.594	1.594

lattice unit. During growth, by repeating this process, kinks at step edges can be "healed". From the point of view of the evolution of two-dimensional islands, this process favours islands of rectangular shape, which has been observed experimentally in the case of Cu [47] and Ni [43]. Downwards step-crossing at kink sites has been discussed by Villarba and Jónsson [88] and Jacobsen et al. [74] in the case of the Pt(111) surface, where the existence of two types of close-packed step give rise to characteristic island shapes. However, to our knowledge, the role of diffusion across step edges at kink sites in the dynamics of surfaces vicinal to the fcc (100) direction has not been studied previously.

Concerning mass transport along step edges "around the corner" created by a kink, we observe that $E_{S2H} < E_{TH} < E_{K2H} < E_{S3H} < E_{K3H} < E_{K3X}$ for all the three metals considered.⁶ Thus hopping is favoured in migration around the corner. Note that K3H (and its reverse process) actually consists of two jumps, denoted by K3H(1) and K3H(2) in Fig. 2, for which the activation barrier of the rate-limiting step is given in Table 2. Some implica-

tions of these results on the interpretation of experiments [89] on diffusion along the step edges in thermodynamic equilibrium in the case of copper have been discussed briefly in Ref. [63]. We also note that there is yet another way of going around the corner by starting from the kink site like in K3H. Namely, the atom can first escape from the kink via process K2H and then proceed to the terrace via S3H and get around the kink by diffusing on the terrace. However, the probability of returning back to the kink site before the jump K2H is very high due to fast diffusion along the straight step edge and the high barrier for the jump S3H. To evaluate the relative importance of mass transport via the terrace in getting around a kink, a theoretical analysis beyond the scope of the present work is required.

⁶ The notion of NA for the process K3X in Table 2 refers to the observation that in the molecular static calculation it is impossible to carry it through (or the reverse process) without constraining more than one degree of freedom and, therefore, the optimal transition path is questionable. With only one constrained degree of freedom, on the other hand, other processes much more expensive than K3H occur.

It is now evident that the effect of kinks on adatom dynamics at steps can be crucial if there is a step edge barrier, and can have far-reaching consequences on growth properties. Even in equilibrium, and already around room temperature, the density of kinks can be considerable, as observed, for example, in STM measurements [89,90]. Studies through growth simulations of the importance of these effects in the presence of a non-negligible step edge barrier at straight step edges are currently in progress [91].

3.4. Many-particle processes at step edges

Having discussed the importance of the concerted two-particle exchange, we shall next consider more complex diffusion processes at step edges, for which we have reported some preliminary results in Ref. [63]. Recently, this topic has also been discussed in the context of flat surfaces. First, in the EAM studies on flat Cu(100) by Black and Tian [92], a considerable number of different many-particle exchange processes were observed around 900 K. Later, Evangelakis and Papanicolaou [29] studied the same system in more detail and extracted the diffusion barriers and prefactors of the various processes observed. However, the energetically favourable diffusion mechanism on the flat fcc (100) surface was clearly simple hopping [29].⁷ Within the basic EMT and other phenomenological descriptions, the occurrence of many-particle diffusion mechanisms can be related to the fact that a major part of the total energy cost comes from breaking nearest-neighbour bonds at the ends of the chain of the moving atoms, while the local configuration in the middle of the chain in the transition state resembles that of a close-packed surface [63]. In the case of a stepped surface studied here, there are two significant differences in energetics compared with diffusion on flat surfaces. First, one end of the chain of the active atoms can be at a step edge, where an atom popping up from the surface can find neighbours to replace some of the broken bonds.

Second, considering mass transport across step edges, the activation barrier for conventional mechanisms can be much higher than that for diffusion on a flat surface. Based on these observations, one can expect a greater relative importance of these processes in the case of stepped surfaces.

To identify the mechanisms relevant to mass transport at step edges, we carried out extensive MD simulations for copper and silver over time-periods of tens of nanoseconds. The temperatures were chosen to satisfy $\exp(-E_{\text{TH}}/k_{\text{B}}T) \approx 0.001$, which for silver, for example, implies $T \approx 650$ K. With this choice, the migration rate of atoms on the surface was large enough to facilitate a reasonable number of independent observations of various diffusion processes. While relatively high compared to typical MBE conditions, this temperature is still low enough to preserve the characteristic structure of the fcc (11 $\bar{1}$) surface and to allow the identification of distinct jumps and exchange processes. Many initial configurations containing various concentrations of kinks and additional adatoms were used.⁸ For example, during a typical single run of length 2.5 ns at $T = 750$ K in the case of Cu, we observed approximately 200 two-particle, 50 three-particle, and ten four-particle processes. Naturally, simple processes such as TH, S1H, S1X, and S2H were commonly observed, as expected.

Concerning the direction perpendicular to steps at straight edges, the three processes E1, E2, and E3 shown in Fig. 2 were most prevalent, the other frequently occurring mechanisms being variations of these. In the process E1, starting from an ideal step edge, two atoms slide together leaving a vacancy behind in the upper terrace. What can follow is that later an adatom diffusing on the upper terrace can move forward to fill the vacancy, so that from the point of view of mass transport one adatom has moved from the upper terrace onto the lower terrace. In such a two-stage process the rate-limiting step is the barrier of E1, which is higher than that of processes S1H and S1X, however.

⁷ Also, many-particle diffusion processes on the Ag(110) surface have been studied in Ref. [93].

⁸ These temperatures are well above the estimated equilibrium roughening temperatures of the fcc (11 $\bar{1}$) surfaces; e.g. see Ref. [94].

In the process E2, diffusion across the whole terrace happens via an atom-by-atom replacement mechanism or, equivalently, by vacancy diffusion. The rate-limiting factor here is the first stage or the barrier E_{K1H} , so that a considerable effective barrier exists for step crossing via E2. Although the activation barrier is rather high, one must bear in mind that this process can be initiated without the prior existence of an adatom or a kink, which increases its probability compared to that of ordinary step-crossing mechanisms such as S1H. Note also that, after diffusing towards the upper step edge, the vacancy very probably gets filled via the kink creation process K1V, leaving the thereby created hole at the upper step edge to be later filled by an adatom. This sequence of events again results in mass transfer across the step edge. When E2 takes place in the opposite direction, the rate-limiting step is the one where the surface atom pops up to the step edge. The barrier for this rate-limiting step can be reduced considerably if there is a kink site into which the atom popping up from the terrace can be absorbed, i.e. for starting the process with and without a kink we find $E_{K2V}^{kv} < E_{E2}^{kv}$ (see Fig. 2).

The mechanism E3 involving a simultaneous transfer of a chain of atoms in the surface layer has the highest activation barrier and, therefore, its observation in our finite-temperature MD simulations must be due to a relatively large prefactor. The barrier for this process is naturally dependent on terrace width; for the corresponding process on the Cu(115) surface we obtain a barrier of 0.97 eV. Another feature characteristic of the process E3 is, due to the similarity of the initial and final configurations, that $E_{E3} = E_{E3}^{kv}$. Some snapshots from MD simulations of processes similar to E2 and E3 on the Cu(119) surface can be found in Ref. [63].

As discussed in the previous sections, the existence of kinks may promote step crossing. Furthermore, combining various vacancy-creation mechanisms with layer-change processes such as K2V provides another possible mechanism for mass transport: step-crossing mediated by vacancy diffusion. For wide terraces, the rate of mass transport via such processes is naturally also

affected by the barrier E_{TV} , which is larger than E_{TH} .⁹ In our finite-temperature MD simulations, processes similar to E1, E2 and E3 resulting in mass transport across step edges were often initiated in the presence of additional kinks suitably located at step edges. We checked the zero-temperature energetics of some of those processes and also similar processes with additional adatoms on the upper terrace; the results do not change the main conclusions made above, however. We also observed a number of complicated many-particle diffusion processes without layer changes close to kink sites or resulting in the creation of kinks at step edges. These processes can be relevant, e.g. to step roughening under equilibrium conditions, but their contribution to mass transport appears to be small.

3.5. The case of an fcc (113) surface

In the special case where two step edges come close to each other to form a (111) microfacet as shown in Fig. 4, the energetics of step crossing changes. This situation is characteristic of the vicinal fcc (113) surface, where even a single kink creates the microfacet. The barriers that in this case differ from those of the higher-index surfaces, are shown in Fig. 4 and listed in Table 3. First, simple hopping and exchange at straight step edges have considerably higher activation barriers than the corresponding processes at fcc (11 m) edges with $m \geq 5$. For Cu(113) and Ni(113), the atomic exchange is actually preferred to hopping. The main difference at kink sites is that the barrier for step crossing by a simple hop (see Fig. 4(c)) is considerably lowered. Thus, in this case kinks enhance step crossing even more than previously.

3.6. Prefactors of the jump rates

As a function of the energy barrier E_M , the prefactors v_M of the jump rates of the activated form display a very simple behaviour as shown in Fig. 5. The dashed curve shows the behaviour corresponding to a one-dimensional cosine poten-

⁹ See footnote 5.

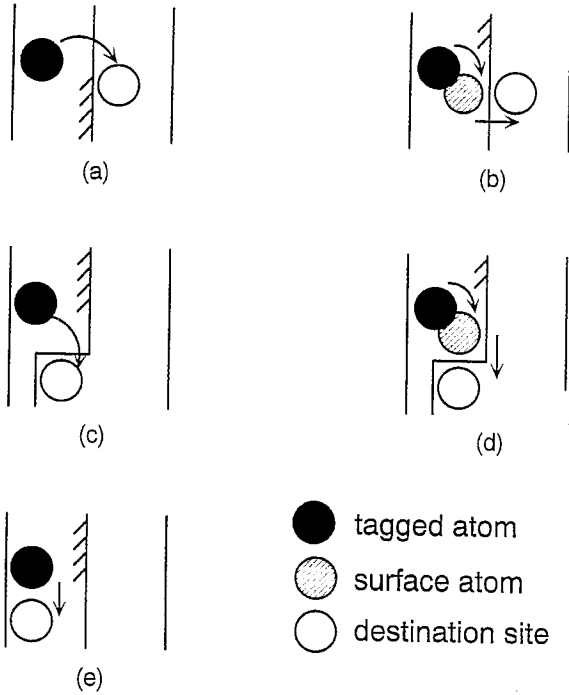


Fig. 4. Some processes available at step edges on the fcc (113) surface.

Table 3

Activation barriers (eV) for some processes occurring on the fcc (113) surface as shown in Fig. 4. All the barriers were evaluated at zero temperature. The process labels in the second column indicate the correspondence to the related processes on higher-index surfaces

Fig. no.	M	Cu		Ag		Ni	
		E_M	E_M^{ev}	E_M	E_M^{ev}	E_M	E_M^{ev}
Fig. 4(a)	S1H(113)	0.889	0.889	0.704	0.704	1.373	1.373
Fig. 4(b)	S1X(113)	0.822	0.822	0.727	0.727	1.302	1.302
Fig. 4(c)	K4Hb(113)	0.283	0.512	0.259	0.433	0.426	0.745
Fig. 4(d)	K4XB(113)	0.553	0.782	0.479	0.652	0.728	1.056
Fig. 4(e)	S2H(113)	0.232	0.232	0.220	0.220	0.351	0.351

tial, $v = \sqrt{E/2l^2m}$, where l is the jump length (here r_{nn}) and m is the atomic mass. The actual values of v_M given by the plotting symbols are somewhat higher, due to the fact that the actual potential has a higher curvature at the bottom of the potential-well corresponding to the initial state, and a slightly lower curvature at the saddle point, which is visible in Fig. 3(b). The full curve shows the fit $v \propto \sqrt{E}$ to the data points. We stress that, in the present study, only prefactors of hopping processes

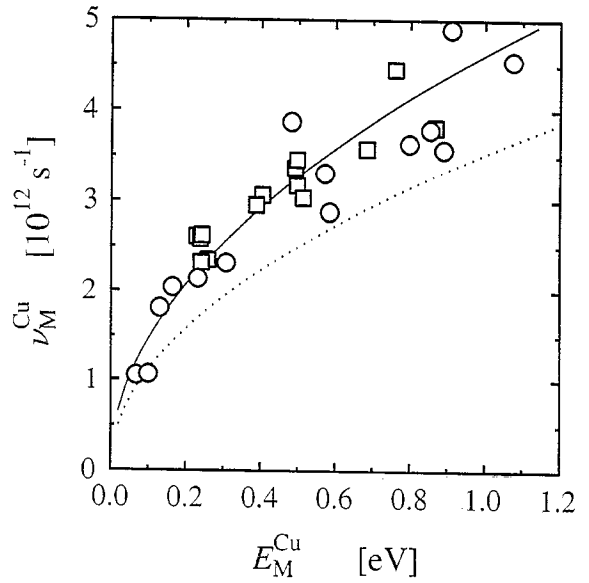


Fig. 5. Behaviour of the prefactor ν_M at zero temperature as a function of the activation barrier E_M for various hopping processes for copper. The squares denote the processes shown in Fig. 6, and circles some other processes at step edges. The dotted curve gives the square root approximation described in the text, and the full curve is a fit to the data shown by the squares.

were considered, with results obtained by the zero-temperature analysis described in the last paragraph of Section 2. While these provide a useful estimate of the microscopic time scales under typical MBE conditions, at higher temperatures the vibrational entropy contribution to the jump rates can have a considerable temperature dependence [95]. Also, recent studies of exchange processes [29,76] indicate that prefactors for them can be several times larger than those for simple hopping

mechanisms. However, at temperatures relevant to most applications in growth phenomena, the activation barrier dominates over the prefactor in determining the actual transition rates.

4. Generic features of diffusion energetics within the EMT

Owing to the popularity of the EMT and other phenomenological methods in studies of diffusion mechanisms, it is useful to consider the generic features and also the limitations of such descriptions in the present context. Considering jumps on terraces and along step edges, the activation barriers E_M fall into a few classes. This is illustrated in Fig. 6, where we show the approximate values of activation barriers for such hopping processes in the most important local configurations in the case of copper. The processes within each class I–V turn out to be characterized by the same values of

two parameters denoted by A and B in Fig. 6. The value of A is one for processes, where the particle in a saddle point configuration is moving along a step edge, and zero otherwise. The value of $B \geq 0$ is the number of nearest-neighbour bonds broken in the process. The activation barriers of the processes shown in Fig. 6 are then very accurately approximated by the formula

$$E \approx E_{\text{TH}} + A \times (E_{\text{S2H}} - E_{\text{TH}}) + B \times (E_{\text{K2H}} - E_{\text{S2H}}). \quad (2)$$

Also, the prefactors ν_M for processes within each class are almost identical.

In Eq. (2), two characteristic properties of the basic EMT and other similar descriptions are displayed. First, the range of interactions is very short so that the possible existence of a new nearest neighbour in the direction of the jump in the final state has only a very small effect (see classes I and II). Second, the energetics can be analysed by using bond-counting arguments, because parameters A and B contain information about the effective coordination number C_{eff} of the jumping atom in the saddle point and in the initial configuration. This can be traced back to the fact that, within the rather narrow range of possible values of C_{eff} on a given surface, the energy of an atom within the EMT is an approximately linear function of C_{eff} , as can be seen in fig. 1 of Ref. [96]. For small changes in the effective coordination, the non-linear part of the energetics, the function F in Eq. (1), can be reasonably well approximated by a linear one, so that bond-counting arguments are indeed reasonable. Although parameterizations other than Eq. (2) could also reproduce the values of E_M reasonably well,¹⁰ we think that, from the point of view of applications, it is useful to distinguish between jumps that transport mass along step edges ($A=1$) and other processes ($A=0$). Note also that, in addition to the processes shown in Fig. 6, several other local geometries for in-plane

class	E_M	A	B	processes
I	0.40	0	0	
II	0.26	1	0	
III	0.50	1	1	
IV	0.76	1	2	
V	0.68	0	1	

Fig. 6. Approximate activation energies E_M and a classification of various in-plane jump processes on the Cu(111) surface. Barriers are given in units of electron-volts. For parameters A and B , see text.

¹⁰ The observation that the activation barriers of various processes fall into a few classes is consistent with EAM results for copper by Karimi et al. [25]. Our explanation for the dependence of E_M on the local environment, as exemplified by Eq. (2), differs somewhat from the one developed by them (see Ref. [97]).

jump processes, e.g. different configurations with additional next-nearest neighbour atoms, are possible; the configurations considered here are those expected to be the most relevant ones from the point of view of mass transport. The energetics of hopping processes across step edges can be understood in a similar way by examining the nature of the initial and saddle point configurations only; e.g. consider the barriers $E_{S1H} \approx E_{K4Hc}$.

Another feature of the EMT description is that after setting the energy scale of nearest and next-nearest neighbour interactions, the rest of the energetics depends on the local geometry of a given diffusion process. This is evident from Fig. 7, where activation barriers of various mechanisms in the case of copper and silver are compared with each other. We find $E_M^{Cu} \approx 1.3 \times E_M^{Ag}$, and a comparison between copper and nickel yields $E_M^{Ni} \approx 1.8 \times E_M^{Ag}$ with a slightly larger scatter around the linear dependence. In addition to the data shown in Tables 1–3, we also determined most of the activation barriers in the case of nickel using a “semi-empirical” parameterization, where in addition to the standard use of the elastic constant C_{44} , the zero-temperature lattice constant and the

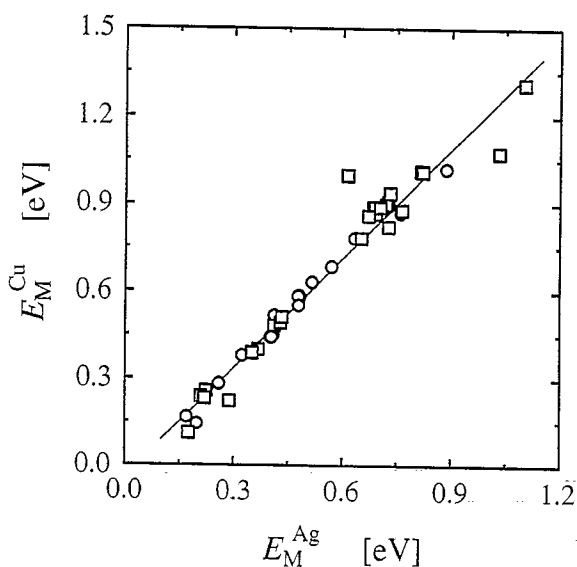


Fig. 7. Comparison of the activation barriers E_M (\circ) and E_M^{Ag} (\square) of the diffusion mechanisms calculated in this work for copper and silver. The straight line is a least-squares fit with a slope of approximately 1.3.

bulk modulus were used as an experimental input.¹¹ The activation barriers given by this second parameter set were mainly larger than those by the standard set, but the relative order of different activation barriers remained largely unchanged. We have also compared our EMT barriers for nickel with the available EAM barriers [19], which turn out to be approximately equal. Further comparison with available results [22,25] given by various phenomenological potentials shows that these models indeed give a very similar description of diffusion processes.

The similarity between EMT and EAM results reflects the fact that these models only contain the coordination-dependent part of energetics, while details of electron structure are not included. As mentioned before, this is a major problem in the case of exchange mechanisms. In the case of aluminium, covalent effects beyond the EMT are known [7] to be responsible for the low activation barrier for exchange on flat (100) surface; for copper a similar effect has been conjectured [75] although the theoretical and experimental evidence is still inconclusive (see Section 3.1), and in the case of silver, exchange down at a straight step edge appears to be much more favourable [34] than predicted by the basic EMT. If overestimating barriers of exchange processes is a generic trend of the basic EMT, then the mechanisms K4X and the various exotic processes introduced in Sections 3.3 and 3.4 could be energetically even more favourable than suggested by our calculations. A study of these processes using more sophisticated approaches would be desirable.

Concerning the application of our results to growth-related problems, Eq. (2) should describe diffusion along step edges rather well, because there are no obvious candidates for exchange processes capable of replacing the jump processes in classes II–V of Fig. 6. In practical simulations, the in-plane processes in class I may need to be replaced by the corresponding simple exchange

¹¹ In the case of copper and silver, corresponding semiempirical parameter sets do not differ very much from those used in this work and were not used in any calculations. For comments concerning the case of nickel, see Ref. [61] and references cited therein. A more recent semiempirical parameter set for EMT can be found in Ref. [66].

processes, possibly with a lower activation barrier. The physics of step-crossings needs some further consideration. The results of Ref. [33] for the process E_{SIX} on silver indicate that, within an ab initio description, the barrier for exchange mechanisms can be much lower than the value given by the EMT, provided that the terrace barrier is not considerably reduced. This possibility must be taken into account in growth models for fcc (100) surfaces, if they are based on activation barriers given by phenomenological potentials.

5. Summary

In this work, we have performed extensive studies of various diffusion mechanisms and the corresponding energy barriers on stepped surfaces vicinal to the (100) surfaces of copper, silver and nickel. We have used the EMT method coupled with finite-temperature MD simulations to examine the role of kinks, vacancies, and many-particle mechanisms in mass transport along and across step edges. Our main conclusions are that in the case of a step edge barrier, kinks at step edges can considerably enhance diffusion across step edges and, in particular, that the barrier at a kink site disappears for an exchange mechanism. Also, for more complicated processes, where step crossing is mediated by vacancy diffusion, the effective barrier for mass transport across steps can be as low as the hopping and exchange mechanisms at a step edge. For very closely spaced steps, such as the (113) facets, these processes may be further enhanced. The implications of these results to the growth properties of (100) surfaces under typical MBE conditions warrant further study.

We have also discussed the generic features of diffusion energetics as given by the EMT and other semi-empirical potentials. Within the accuracy of such descriptions, the results for the activation barriers for hopping mechanisms are very similar. This is due to the fact that in these mechanisms the dominant part of the energy cost can be related to the change in the effective coordination number of the jumping atom and its neighbours during the process. The main limitation of the present and related studies lies in the role of the exchange

processes, in particular near step edges. Recently, first-principles calculations have shown that, at least for silver, exchange can remove the static step edge barrier. This cannot be reliably estimated by the phenomenological methods, and must be taken into account if realistic growth models for MBE homoepitaxy are being constructed. However, the low value for the exchange near a kink site found in the present study suggests that this mechanism may play an even more important role than expected. First-principles calculations of such processes would be most interesting.

Acknowledgements

This work is in part supported by the Academy of Finland. J.M. is supported by the Academy of Finland, the Emil Aaltonen Foundation, and the Finnish Cultural Foundation. I.V. thanks the Neste Co. Foundation and the Jenny and Antti Wihuri Foundation for support. Finally, computing resources at the University of Helsinki, Center for Scientific Computing, and the University of Jyväskylä in Finland are gratefully acknowledged.

References

- [1] V.T. Binh (Ed.), *Surface Mobilities on Solid Materials: Fundamental Concepts and Applications*, Plenum, New York, 1981.
- [2] G. Godreche (Ed.), *Solids Far from Equilibrium*, Cambridge University Press, Cambridge, 1991. A.-L. Barabasi, H.E. Stanley, *Fractal Concepts in Surface Growth*, Cambridge University Press, Cambridge, 1995.
- [3] E.W. Müller, *Z. Phys.* 131 (1951) 136.
- [4] G. Binnig, H. Rohrer, Ch. Gerber, E. Weibel, *Phys. Rev. Lett.* 49 (1982) 575.
- [5] G. Wahnström, *Surf. Sci.* 159 (1985) 311; *Surf. Sci.* 164 (1985) 449; *Phys. Rev. B* 33 (1986) 1020. R. Gomer, *Rep. Prog. Phys.* 53 (1990) 917. T. Ala-Nissila, S.C. Ying, *Prog. Surf. Sci.* 39 (1992) 227. L.Y. Chen, S.C. Ying, *Phys. Rev. Lett.* 71 (1993) 4361; *Phys. Rev. B* 49 (1994) 13838. R. Ferrando, G. Tréglia, *Phys. Rev. B* 50 (1994) 12104; *Phys. Rev. Lett.* 76 (1996) 2109. R. Ferrando, *Phys. Rev. Lett.* 76 (1996) 4195.
- [6] G.L. Kellogg, P.J. Feibelman, *Phys. Rev. Lett.* 64 (1990) 3143.
- [7] P.J. Feibelman, *Phys. Rev. Lett.* 65 (1990) 729.

- [8] G.L. Kellogg, Surf. Sci. 246 (1991) 31; Surf. Sci. 266 (1992) 18.
- [9] X.D. Xiao, Y. Xie, C. Jakobsen, H. Galloway, M. Salmeron, Y.R. Shen, Phys. Rev. Lett. 74 (1995) 3860.
- [10] C. Uebing, R. Gomer, Surf. Sci. 306 (1994) 419; Surf. Sci. 306 (1994) 427; Surf. Sci. 317 (1994) 165.
- [11] J. Merikoski, S.C. Ying, Surf. Sci. 381 (1997) L623.
- [12] R.L. Schwoebel, E.J. Shipsey, Appl. J. Phys. 37 (1966) 3682. G. Ehrlich, F.G. Hudda, J. Chem. Phys. 44 (1966) 1039. R.L. Schwoebel, J. Appl. Phys. 40 (1969) 614.
- [13] J. Villain, J. Phys. I 1 (1991) 19.
- [14] J. Krug, M. Plischke, M. Siegert, Phys. Rev. Lett. 70 (1993) 3271. J. Krug, H.T. Dobbs, Phys. Rev. Lett. 73 (1994) 1947.
- [15] M.D. Johnson, C. Orme, A.W. Hunt, D. Graff, J. Sudijono, L.M. Sander, B.G. Orr, Phys. Rev. Lett. 72 (1994) 116.
- [16] J.A. Meyer, J. Vrijmoeth, H.A. van der Vegt, E. Vlieg, R.J. Behm, Phys. Rev. B 51 (1995) 14790.
- [17] K.W. Jacobsen, J.K. Nørskov, M.J. Puska, Phys. Rev. B 35 (1987) 7423. K.W. Jacobsen, Comments Condens. Matter Phys. 14 (1988) 129.
- [18] C.-L. Liu, J.M. Cohen, J.B. Adams, A.F. Voter, Surf. Sci. 253 (1991) 334.
- [19] C.-L. Liu, J.B. Adams, Surf. Sci. 265 (1992) 262.
- [20] Z.J. Tian, T.S. Rahman, Phys. Rev. B 47 (1993) 9751.
- [21] R.C. Nelson, T.L. Einstein, S.V. Khare, P.J. Rous, Surf. Sci. 295 (1993) 462.
- [22] P. Stoltze, J. Phys.: Condens. Matter 6 (1994) 9495.
- [23] C.-L. Liu, Surf. Sci. 316 (1994) 294.
- [24] M. Breeman, G.T. Barkema, D.O. Boerma, Surf. Sci. 303 (1994) 25.
- [25] M. Karimi, T. Tomkowski, G. Vidali, O. Biham, Phys. Rev. B 52 (1995) 5364.
- [26] C.-L. Liu, Int. J. Mod. Phys. B: 9 (1995) 1.
- [27] U. Kürpick, T.S. Rahman, in: Surface Diffusion: Atomistic and Collective Processes, NATO ASI Series, in press.
- [28] Z.-P. Shi, Z. Zhang, A.K. Swan, J.F. Wendelken, Phys. Rev. Lett. 76 (1996) 4927.
- [29] G.A. Evangelakis, N.I. Papanicolaou, Surf. Sci. 347 (1996) 376.
- [30] G. Boisvert, L.J. Lewis, Phys. Rev. B 54 (1996) 2880.
- [31] C. Lee, G.T. Barkema, M. Breeman, A. Pascuarello, R. Car, Surf. Sci. 306 (1994) L575.
- [32] G. Boisvert, L.J. Lewis, M.J. Puska, R.M. Nieminen, Phys. Rev. B 52 (1995) 9078.
- [33] B.D. Yu, M. Scheffler, Phys. Rev. Lett. 77 (1996) 1095.
- [34] B.D. Yu, M. Scheffler, preprint cond-mat/9612005, 1996.
- [35] P.T. Tung, W.R. Graham, Surf. Sci. 97 (1980) 73.
- [36] P. Schrammen, J. Hölzl, Surf. Sci. 130 (1983) 203.
- [37] J.J. DeMiguel, A. Sánchez, A. Cebollada, J.M. Gallego, J. Ferrón, S. Ferrer, Surf. Sci. 189–190 (1987) 1062.
- [38] S.T. Purcell, B. Heinrich, A.S. Arrott, Phys. Rev. B 35 (1987) R6458.
- [39] Y. Suzuki, H. Kikuchi, N. Koshizuka, Jpn. J. Appl. Phys. 27 (1988) L1175.
- [40] H.J. Ernst, F. Fabre, J. Lapujoulade, Phys. Rev. B 46 (1992) R1929; Surf. Sci. 275 (1992) L682.
- [41] M. Poensgen, J.F. Wolf, J. Frohn, M. Giesen, H. Ibach, Surf. Sci. 274 (1992) 430.
- [42] M. Breeman, D.O. Boerma, Surf. Sci. 269–270 (1992) 224.
- [43] E. Kopatzki, S. Günther, W. Nichtl-Pecher, R.J. Behm, Surf. Sci. 284 (1993) 154.
- [44] H.-J. Ernst, F. Fabre, R. Folkerts, J. Lapujoulade, J. Vac. Sci. Technol. A: 12 (1994) 1809.
- [45] H.-J. Ernst, F. Fabre, R. Folkerts, J. Lapujoulade, Phys. Rev. Lett. 72 (1994) 112.
- [46] H.A. van der Vegt, M. Breeman, S. Ferrer, V.H. Etgens, X. Torrelles, P. Fajardo, E. Vlieg, Phys. Rev. B 51 (1995) R14806.
- [47] H. Dürr, J.F. Wendelken, J.-K. Kuo, Surf. Sci. 328 (1995) L527.
- [48] M.H. Langelaar, M. Breeman, D.O. Boerma, Surf. Sci. 352–354 (1996) 597.
- [49] W.C. Elliott, P.F. Miceli, T. Tse, P.W. Stephens, Physica B 221 (1996) 65; Phys. Rev. B 54 (1996) 17938.
- [50] P. Hohenberg, W. Kohn, Phys. Rev. B 136 (1964) 864. W. Kohn, L.J. Sham, Phys. Rev. 140 (1965) A1133.
- [51] J.P. Perdew, J.A. Chevary, S.H. Vosko, K.A. Jackson, M.R. Pederson, D.J. Singh, C. Fiolhais, Phys. Rev. B 46 (1992) 6671 and references therein.
- [52] M.S. Daw, M.I. Baskes, Phys. Rev. B 29 (1984) 6443. S.M. Foiles, M.I. Baskes, M.S. Daw, Phys. Rev. B 33 (1986) 7983.
- [53] R.P. Gupta, Phys. Rev. B 23 (1981) 6265. V. Rosato, M. Guillope, B. Legrand, Philos. Mag. A 59 (1989) 321.
- [54] M.W. Finnis, J.E. Sinclair, Philos. Mag. A: 50 (1984) 45.
- [55] F. Ercolessi, E. Tosatti, M. Parrinello, Phys. Rev. Lett. 57 (1986) 719. F. Ercolessi, M. Parrinello, E. Tosatti, Philos. Mag. A: 58 (1988) 213.
- [56] P. Stoltze, J.K. Nørskov, U. Landman, Phys. Rev. Lett. 61 (1988) 440.
- [57] H. Häkkinen, M. Manninen, Phys. Rev. B 46 (1992) 1725.
- [58] H. Häkkinen, J. Merikoski, M. Manninen, J. Timonen, K. Kaski, Phys. Rev. Lett. 70 (1993) 2451.
- [59] P.A. Gravil, S. Holloway, Phys. Rev. B 53 (1996) 11128.
- [60] K.W. Jacobsen, J.K. Nørskov, Phys. Rev. Lett. 60 (1988) 2496.
- [61] H. Häkkinen, J. Merikoski, M. Manninen, J. Phys.: Condens. Matter 3 (1991) 2755.
- [62] P. Stoltze, J.K. Nørskov, Phys. Rev. B 48 (1993) 5607.
- [63] J. Merikoski, T. Ala-Nissila, Phys. Rev. B 52 (1995) R8715.
- [64] S. Liu, H. Metiu, Surf. Sci. 359 (1996) 245.
- [65] M.J. Puska, in: R.M. Nieminen, M.J. Puska, M.J. Manninen (Eds.), Many-Atom Interactions in Solids, Springer, Berlin, 1990, p. 134.
- [66] K.W. Jacobsen, P. Stoltze, J.K. Nørskov, Surf. Sci. 366 (1996) 394.
- [67] H. Häkkinen, M. Manninen, J. Phys.: Condens. Matter 1 (1989) 9765.
- [68] W.G. Hoover, Phys. Rev. A 31 (1985) 1695.
- [69] S. Nosé, J. Chem. Phys. 81 (1984) 511.

- [70] B.L. Holian, A.F. Voter, R. Ravelo, *Phys. Rev. E*: 52 (1995) 2338.
- [71] A. Cucchetti, S.C. Ying, *Phys. Rev. B* 54 (1996) 3300.
- [72] P. Hänggi, P. Talkner, M. Borkovec, *Rev. Mod. Phys.* 62 (1990) 251.
- [73] D.E. Sanders, A.E. Depristo, *Surf. Sci.* 260 (1992) 116.
- [74] J. Jacobsen, K.W. Jacobsen, P. Stoltze, J.K. Nørskov, *Phys. Rev. Lett.* 74 (1995) 2295.
- [75] L. Hansen, P. Stoltze, K.W. Jacobsen, J.K. Nørskov, *Phys. Rev. B* 44 (1991) 6523.
- [76] L.B. Hansen, P. Stoltze, K.W. Jacobsen, J.K. Nørskov, *Surf. Sci.* 289 (1993) 68.
- [77] L.S. Perkins, A.E. DePristo, *Surf. Sci.* 325 (1995) 169.
- [78] L.S. Perkins, A.E. DePristo, *Surf. Sci.* 294 (1993) 67.
- [79] J.G. Amar, F. Family, *Phys. Rev. Lett.* 77 (1996) 4584.
- [80] G. Ehrlich, *Surf. Sci.* 331–333 (1995) 865.
- [81] R. Stumpf, M. Scheffler, *Phys. Rev. Lett.* 72 (1994) 254.
- [82] J.W. Evans, M.C. Bartelt, *J. Vac. Sci. Technol. A*: 12 (1994) 1800.
- [83] G.L. Kellogg, *Surf. Sci.* 359 (1996) 237.
- [84] T. Michely, M. Hohage, M. Bott, G. Comsa, *Phys. Rev. Lett.* 70 (1993) 3943.
- [85] H. Röder, K. Bromann, H. Brune, K. Kern, *Phys. Rev. Lett.* 74 (1995) 3217.
- [86] G.T. Barkema, O. Biham, M. Breeman, D.O. Boerma, G. Vidali, *Surf. Sci.* 306 (1994) L569.
- [87] C. Chen, T.T. Tsong, *Phys. Rev. B* 47 (1993) 15852.
- [88] M. Villarba, H. Jónsson, *Phys. Rev. B* 49 (1994) 2208.
- [89] M. Giesen-Seibert, R. Jentjens, M. Poensgen, H. Ibach, *Phys. Rev. Lett.* 71 (1993) 3521. M. Giesen-Seibert, F. Schmitz, R. Jentjens, H. Ibach, *Surf. Sci.* 329 (1995) 47.
- [90] L. Kuipers, M.S. Hoogeman, J.W.M. Frenken, *Phys. Rev. Lett.* 71 (1993) 3517.
- [91] J. Merikoski et al., unpublished results, 1997.
- [92] J.E. Black, Z.-J. Tian, *Phys. Rev. Lett.* 71 (1993) 2445.
- [93] R. Ferrando, *Phys. Rev. Lett.* 76 (1996) 4195.
- [94] B. Salanon, F. Fabre, J. Lapujoulade, W. Selke, *Phys. Rev. B* 38 (1988) 7385.
- [95] U. Kürpick, A. Kara, T.S. Rahman, *Phys. Rev. Lett.* 78 (1997) 1086.
- [96] J. Merikoski, H. Häkkinen, M. Manninen, J. Timonen, K. Kaski, *Phys. Rev. B* 49 (1994) 4938.
- [97] O. Biham, M. Karimi, G. Vidali, R. Kennett, H. Zeng, preprint cond-mat/9611095.